The Yeast Nucleoporin Nup188p Interacts Genetically and Physically with the Core Structures of the Nuclear Pore Complex

Ulf Nehrbass,* Michael P. Rout,* Shawna Maguire,‡ Günter Blobel,* and Richard W. Wozniak‡

*The Laboratory of Cell Biology, Howard Hughes Medical Institute, The Rockefeller University, New York 10021; and ‡Department of Anatomy and Cell Biology, University of Alberta, Edmonton, AB, Canada T6G 2H7

Abstract. We have isolated a major protein constituent from a highly enriched fraction of yeast nuclear pore complexes (NPCs). The gene encoding this protein, Nup188p, was cloned, sequenced, and found to be nonessential upon deletion. Nup188p cofractionates with yeast NPCs and gives an immunofluorescent staining pattern typical of nucleoporins. Using immunoelectron microscopy, Nup188p was shown to localize to both the cytoplasmic and nucleoplasmic faces of the NPC core. There, Nup188p interacts with an integral protein of the pore membrane domain, Pom152p, and another abundant nucleoporin, Nic96p. The effects of various mutations in the *NUP188* gene on the structure of the nuclear envelope and the function of the NPC were examined. While null mutants of *NUP188* appear normal, other mutants allelic to *NUP188* exhibit a dominant effect leading to the formation of NPC-associated nuclear envelope herniations and growth inhibition at 37°C. In addition, depletion of the interacting protein Pom152p in cells lacking Nup188p resulted in severe deformations of the nuclear envelope. We suggest that Nup188p is one of a group of proteins that form the octagonal core structure of the NPC and thus functions in the structural organization of the NPC and nuclear envelope.

NUCLEOPORINS are the molecular constituents of the nuclear pore complex (NPC)[1]. Approximately 50 such individual nucleoporins (Rout and Blobel, 1993) constitute the complex 100 MD NPC structure and mediate multiple nuclear translocation processes. The core of the NPC reveals an octagonally symmetric architecture with several repetitious structural elements such as spokes, rings, and radial arms surrounding a central tube (termed "central plug") (Akey and Radermacher, 1993; Hinshaw et al., 1992). Filamentous structures attached to the core appear asymmetric with linear filaments extending into the cytoplasm and a nuclear cage projecting into the nucleoplasm (Unwin and Milligan, 1982; Jarnik and Aebi, 1991; Goldberg et al., 1992; Ris and Malecki, 1993). The nucleoporins so far characterized in yeast fall into two subgroups: those that contain repetitive peptide motifs (GLFG, XFXFG, or FG) and those that do not (for review see Rout and Wente, 1994; Doye et al., 1994; Kraemer et al., 1995; Gorsch et al., 1995; Grandi et al., 1995; Hurwitz and Blobel 1995; Pemberton et al., 1995; Li et al., 1995; Aitchison et al., 1995*a*,*b*; Heath et al., 1995). Among the nonrepeat nucleoporins is a further subgroup of major proteins including Nup170p, Nup157p, Nic96p, and the pore membrane protein Pom152p (Grandi et al., 1993; Wozniak et al., 1994; Aitchison et al., 1995*a*), which appear more abundant than the other constituents.

Repeat-containing nucleoporins are directly involved in the mechanics of nuclear translocation. In vitro assays have established that the repetitive peptide domains of these nucleoporins are docking sites for soluble transport factors (Radu et al., 1995; Moroianu et al., 1995; Kraemer et al., 1995; Rexach and Blobel, 1995; Iovine et al., 1995). This observation is in accordance with the inhibition of specific nuclear transport functions associated with repeat nucleoporin mutants in vivo (reviewed in Rout and Wente, 1994; Fabre and Hurt, 1994). However, mutations in repeat nucleoporins not only affect transport processes, but can also cause structural defects such as NPC clustering and massive distortions of the nuclear morphology. It has therefore not been possible to distinguish between nucleoporins involved in transport and those responsible for the structural organization of the NPC, since both functions are closely intertwined (reviewed in Rout and Wente, 1994; Doye et al., 1994; Pemberton et al., 1994; Gorsch et al., 1995; Aitchison et al., 1995*a*,*b*).

With this background, further understanding of NPC function hinges on integrating subgroups of nucleoporins into the context of known NPC substructures. Apart from Pom152p (Wozniak et al., 1994), a major nonrepeat protein located in the nuclear pore-membrane domain of the nuclear envelope (NE) (and thus termed a pom), and Nup159p, a repeat nucleoporin (Kraemer et al., 1995; Gorsch

U. Nehrbass and S. Maguire contributed equally to this work.

Please address all correspondence to Richard W. Wozniak, Department of Anatomy and Cell Biology, 5-14 Medical Sciences Building, University of Alberta, Edmondton, Alberta, Canada T6G 2H7. Tel.: (403) 492-1384; Fax: (403) 492-0450; e-mail: rwozniak@anat.med.ualberta.ca.

1. *Abbreviations used in this paper*: HA, hemagglutinin; NE, nuclear envelope; NPC, nuclear pore complex; ORF, open reading frame.

et al., 1995) that is exposed at the cytoplasmic face of the NPC, as yet no other NPC protein has been sublocalized in yeast. Some progress has been made in defining biochemical subcomplexes within the NPC through nearest neighbor analysis. One such subcomplex containing three repeat- (Nup49p, Nup57p, Nsp1p) and one nonrepeat nucleoporin, Nic96p (Grandi et al., 1995), has been identified in yeast. However, this subcomplex remains to be sublocalized within the NPC.

Here, we report the identification and characterization of a novel major nucleoporin, Nup188p. We demonstrate that Nup188p is located to both the nucleo- and the cytoplasmic faces of the NPC core, where it interacts genetically and physically with the pore membrane protein Pom152p. We show that Nup188p function is required for the structural integrity of the NPC and the NE. This function is integrated with that of the other major nonrepeat nucleoporins, as reflected by their genetic interactions. We propose that Nup188p is part of a subgroup of major nonrepeat nucleoporins that together are part of the NPC core.

Materials and Methods

Yeast Manipulations and Plasmids

The strains used in this work are listed in Table I. All yeast manipulations were performed as outlined in Aitchison et al. (1995*a*). The plasmids used in this study have been previously described in Wozniak et al. (1994) and Aitchison et al. (1995*a*) with the following exceptions: p33, pSB32 (*LEU2*) containing the *NUP188* locus; YepH and YepW (Wimmer et al., 1992); pNUP188, pUN100 that contains a genomic HindIII/BamHI fragment including the *NUP188* gene; pNUP188CB, pUN100 (*CEN/LEU2*) containing *NUP188* in which the STOP codon has been substituted by a BamHI restriction site (see below); pNUP188PA and pNUP188BPA, pUN100 (*CEN/LEU2*) containing protein A–tagged *NUP188* (PA) or a truncated version of *NUP188* tagged with protein A (BPA; see below); pPOM152-HAH, the plasmid pPM1-HA to which the coding sequence of six histidine residues was added to the 3′ end of the *POM152* open reading frame (ORF); pPOM152-H, the plasmid pPOM152 to which the coding sequence of six histidine residues was added to the 3′ end of the *POM152* ORF; pBlueNUP188; pBluescript (Stratagene Cloning Systems, La Jolla, CA) containing a genomic HindIII/BamHI fragment including *NUP188*.

Isolation and Complementation of POM152 Synthetic Lethal (PSI) Mutants Allelic to NUP188

Mutants dependent on a plasmid-born copy of *POM152* were isolated using a colony-sectoring assay described in Aitchison et al. (1995*a*). From this screen, 32 sec^-, 5-FOA_S mutants were isolated and shown to be recessive. Using approaches previously described (Aitchison et al., 1995*a*), analysis of the mutant strain ps144 revealed that its sec^-/5-FOA_S phenotype appeared to be associated with a single gene. To isolate the corresponding wild-type allele, ps144 was transformed with a yeast genomic library in pSB32 (*CEN/LEU2*) as described (Aitchison et al., 1995*a*), and 16 complementing plasmids were isolated. Restriction analysis revealed that the plasmids contained one of three separate but overlapping inserts. Inserts were partially sequenced. Each insert contained the *NUP188* ORF. To examine the ability of *NUP188* to complement the remaining *psl* mutants, the plasmid p33 was introduced into the remaining psl strains by electroporation. Transformants were scored for growth on 5-FOA–containing plates. Those mutants complemented by *NUP188* were crossed with NP188/PM152 (*pom152Δnup188Δ*, see below). All of the resulting

Table I. Yeast Strain Genotype

Strain	Genotype	Derivation
ps14	*Matα ade2 ade3 ura3 his3 trp1 leu2 can1 pom152-2::HIS3 nup188-4 pCH1122-POM152(ADE3-URA3)*	Synthetic lethal derived from PM152-CP (Aitchison et al., 1995*a*)
ps144	*Matα ade2 ade3 ura3 his3 trp1 leu2 can1 pom152-2::HIS3 nup188-44 pCH1122-POM152(ADE3-URA3)*	Synthetic lethal from PM152-CP
NP188Δ	*Mata/Matα ade 2-1/ade2-1 ura3-1/ura3-1 his3-11,15/his3-11,15 trp1-1/trp1-1 leu2-3,112/leu2-3,112 can1-100/can1-100 nup188-1::HIS3/+*	Integrative transformation of W303 with linearized p33::HIS3
Y28	*Mata ade2-1 ura3-1 trp1-1 leu 2-3 can1-100 nup188-2::HIS3*	see Materials and Methods
CSL5	*Matα ade2-1 ura3-1 leu2-3 can1 pom152-2::HIS3 nup 188-3::TRP1 pYEUra3-POM152 (URA3)*	see Materials and Methods
NP188PA	*Mata ade2-1 ura3-1 trp1-1 leu 2-3 can1-100 nup188-2::HIS3 pNUP188PA (LEU2)*	Y28 transformed with pNUP188PA
NP188BPA	*Mata ade 2-1 ura3-1 trp1-1 leu 2-3 can1-100 nup 188-2::HIS3 pNUP 188BPA (LEU2)*	Y28 transformed with pNUP188BPA
P7AB-1	*Mata/Matα ade2-1/ade2-1 ura3-1/ura3-1 his3-11,15/his3-11,15 trp1-1/trp1-1 leu2-3,112/leu2-3,112 can1-100/can1-100 pom152-2::HIS3/pom152-2::HIS3 pom152-1 (LEU2)*	
NP188-2.4	*Matα ade2-1 ura3-1 his3-11,15 trp1-1 leu2-3,112 can1-100 nup188-1::HIS3*	Segregant of sporulated NP188Δ
P7AB-B61H	*Mata/Matα ade2-1/ade2-1 ura3-1/ura3-1 his3-11,15/his3-11,15 trp1-1/trp1-1 leu2-3,112/leu2-3,112 can1-100/can1-100 pom152-2::HIS3/pom152-2::HIS3 pPOM152-HAH (LEU2)*	

diploid strains, including those derived from ps14 and ps144, failed to grow on 5-FOA–containing plates, suggesting the mutants are allelic to *NUP188*.

Construction of NUP188 Null Mutations and the CSL5 Strain

We have deleted and disrupted the *NUP188* gene by integrative transformation using the procedure of Rothstein (1991). The majority of the *NUP188* ORF was deleted by removing a NcoI/XbaI fragment from the plasmid p33 and replacing it with the *HIS3* marker gene derived from pJJ215 (Jones and Prakash, 1990). The resulting plasmid (p33::HIS3) was linearized and transformed into the diploid strain W303 (Aitchison et al., 1995*a*). His^+ transformants were selected on synthetic media (SM)-histidine plates, and heterozygous diploids carrying the *nup188::HIS3* disruption were identified by Southern blotting. A null strain, NP188Δ, was sporulated and tetrads were dissected. All of the resulting spores were viable and displayed a 2:2 segregation of the *HIS3* marker. Southern blotting confirmed that the His^+ haploids contained only the disrupted copy of *NUP188*.

Two additional disruptions of the *NUP188* gene were also performed using procedures similar to those described for NP188Δ. The *TRP1* and *HIS3* marker genes were PCR amplified from the plasmids YepW and YepH, respectively, using primers containing 5′ EcoRI sites. The resulting products were used to replace an internal 4.5-kb EcoRI fragment, the *NUP188* ORF encoding to amino acid residues 99–1612 in the plasmid pBlueNUP188. The *nup188::HIS3* construct was used to disrupt a chromosomal copy of *NUP188* in the diploid strain W303. From the resulting cells, a haploid strain (Y28) containing the *nup188::HIS3* was isolated. To create the CSL5 strain, the *nup188::TRP1* disruption construct was transformed into a haploid strain PM152-75 (*pom152Δ*; Aitchison et al., 1995*a*) carrying *POM152* under the control of the *GAL1* promoter in the plasmid pYEUra3-POM152 (Wozniak et al., 1994). Transformants were selected on galactose medium lacking tryptophan, and homologous integrations verified by Southern blotting.

Isolation and Peptide Sequence of Nup188p

Fractions derived from the SDS-hydroxylapatite chromatography of isolated yeast NPCs and containing the 170-kD species were pooled (corresponding to fraction 50–54 in Fig. 3 of Wozniak et al., 1994), and the polypeptide constituents were separated by SDS-PAGE. This gel revealed a closely spaced doublet at ~170 kD (see Fig. 1 *A*). Polypeptides were electrophoretically transferred to polyvinyldifluoride membrane, visualized with 0.1% Ponceau red (in 1% acetic acid), and the faster migrating species was excised. Several internal peptides were sequenced using previously described procedures (Wozniak et al., 1994).

Isolation and Sequencing of the NUP188 Gene

The sequence of a peptide fragment derived from the faster migrating species of a prominent 170-kD double band on SDS-PAGE was used to design a pair of degenerate sense and antisense oligonucleotide primers encoding amino acid residues YLNSRI (residues 1611–1616 of Nup188p) and QQQLED (residues 1624–1629 of Nup188p), respectively. Following the method of Lee et al. (1988), these primers and *Saccharomyces cerevisiae* genomic DNA (Promega, Madison, WI) were used to PCR amplify the cDNA segment encoding the 19–amino acid residue peptide. From the sequence of the PCR product an oligonucleotide was designed corresponding to the nucleotide sequence between the primers. The oligonucleotide was labeled with γ-[^{32}P]ATP using polynucleotide kinase (Boehringer Mannheim, Mannheim, Germany) and used to screen a *S. cerevisiae* genomic library in plasmid Ycp50 (Rose et al., 1987) as described (Ausubel et al., 1992). Two clones were isolated. Plasmids derived from these clones contained overlapping inserts encoding a deduced ORF of 1655 amino-acid residues.

Production of Nup188p- and Nup170p-specific Antiserum

A cDNA fragment encoding 59- and 56-kD segments of Nup188p (amino acid residues 1041–1613) and Nup170p (amino-acid residues 697–1207), respectively, were synthesized using PCR and each fused to the 3′ end of the IgG binding domains of *Staphylococcus aureus* protein A in the prokaryotic expression vector pRIT2T (Pharmacia Biotech Inc., Piscataway, NJ). Expression and purification of the resulting fusion proteins on IgG-Sepharose 6 fast flow (Pharmacia), were performed as described by the manufacturer. The purified protein A fusion proteins were used to elicit antibodies in rabbits, and the specificity of the resulting antiserum was examined by immunoblotting. Procedures for the blocking, probing (with anti-Nup188p), and the detection of antibody binding with the ECL detection system were performed essentially as instructed by the manufacturer (Amersham, Arlington Heights, IL).

Epitope Tagging of NUP188

DNA encoding five IgG-binding repeat units of *S. aureus* protein A were PCR amplified as described in Schnell and Blobel (1993), with the modification that the PCR primers contained 5′ BamHI restriction sites. The STOP codon of the *NUP188* gene in the plasmid pNUP188 was replaced by a BamHI site. This was achieved by PCR amplifying the 3′ 1030-bp of *NUP188* using the sense primer 5′ GAGATTGACTTTATTAAA 3′ and the antisense primer 5′ TTAGGATCCAACGTCCTTAAATAGTGA 3′ containing a 5′ BamHI site. This PCR amplified fragment was digested with restriction enzymes BglII and BamHI, and cloned into vector pNUP188, which had been digested with BglII and BamHI, thus releasing a 1-kb region of the *NUP188* ORF including the STOP codon plus the 2.2-kb sequence downstream of *NUP188*. The resulting plasmid carrying *NUP188* with a BamHI site instead of the STOP codon was termed pNUP188CB. Plasmid pNUP188CB was then digested with BamHI and a PCR-amplified, BamHI-digested DNA fragment coding for the IgG-binding repeats of protein A was cloned into this novel BamHI site at the 3′ end of *NUP188* to create plasmid pNUP188PA. Alternatively, the IgG repeats were cloned into the plasmid pNUP188CB after digestion with BglII and BamHI, thus truncating the *NUP188* at the BglII site and inserting protein A. The resulting plasmid was termed pNUP188BPA. Plasmids were transformed into a haploid *nup188Δ* yeast strain (Y28) for expression.

Preparation of Yeast Extracts and Western Blot Analysis

Whole-cell yeast extracts were prepared as described by Wozniak et al. (1994). Yeast subcellular fractionation leading to the isolation of NPCs was performed as described by Rout and Blobel (1993). For Western blot analysis, proteins were separated by SDS-PAGE and then transferred electrophoretically onto nitrocellulose. Blots were probed with mAb118C3 (anti-Pom152p) as described (Strambio-de-Castillia et al., 1995).

Immunoprecipitation of Pom152p-HA

NEs were isolated from two yeast strains, P7AB-B61H (synthesizing hemagglutinin antigen [HA]-tagged Pom152p; Pom152p-HA) and P7AB-1 (lacking the HA tag), using the procedure of Strambio-de-Castillia et al. (1995). All of the following procedures were conducted at 4°C. NEs derived from 50 OD_{260} U of isolated nuclei were suspended in 0.5 ml of 10 mM bisTris, pH 6.5, 0.1 mM $MgCl_2$, 0.2 mM PMSF. NEs were then disrupted with an equal volume of 2× solubilization buffer (1× being 25 mM NaCl, 2% Triton X-100, 1 mM EDTA, 25 mM Tris, pH 8.0, 0.01 mM DTT, 0.5 mM PMSF). After a 15-min incubation on ice, samples were centrifuged (90,000 *g* for 5 min), and the supernatant fraction was then preabsorbed with 1 μl mouse serum for 1 h followed by the addition of 50 μl of protein G–Sepharose 4 beads (Pharmacia Biotech Inc., Piscataway, NJ) for an additional hour to reduce nonspecific binding. An mAb (12CA5) directed against the HA tag (1 μl ascites fluid; Berkeley Antibody Co., Richmond, CA) was then added to the precleared NE extract and incubated for 3 h. Immune complexes were absorbed on 50 μl of protein G–Sepharose 4 beads, washed extensively with solubilization buffer, and eluted with 0.5 M acetic acid, pH 3.4. Aliquots of the starting nuclear extract, the eluted fraction, and the unbound fraction were then analyzed by SDS-PAGE, and Western blotting was performed as described above.

Indirect Immunofluorescence and Electron Microscopy

Immunofluorescence was performed as described by Kilmartin and Adams (1984) with modifications (Wente et al., 1992; Aitchison et al., 1995*a*).

For electron microscopy, cells were harvested in midlog phase, washed, and then fixed as described in Aitchison et al. (1995*a*). For the Pom152p depletion experiments, CSL5 cells were grown in raffinose-containing medium (1% yeast extract, 2% bactopeptone, 2% raffinose) to midlogarithmic phase before washing and incubation in YPGal or YPD medium.

Preembedding labeling immunoelectron microscopy was performed on

nuclear envelopes from the strain NP188PA essentially as described by Kraemer et al. (1995) with the following modifications. After primary fixation, envelopes were incubated overnight at 4°C with IEM buffer containing a 1:20 dilution of affinity-purified rabbit IgG (preabsorbed against yeast cells fixed for immunofluorescence microscopy [Kilmartin and Adams, 1984]). After washing, the bound antibody was visualized with an overnight incubation of a 1:10 dilution of 10-nm gold anti-rabbit IgG (Sigma Chemical Co., St. Louis, MO) in IEM buffer.

Results

Nup188p Is a Major Yeast Nucleoporin

Nucleoporins that form the repeating subunits of the NPC rings and spokes are expected to be abundant constituents of the isolated NPC fraction. SDS-PAGE analysis of the protein constituents of isolated yeast nuclear pore complexes (Rout and Blobel, 1993) reveals several major polypeptides (Rout and Blobel, 1993; Wozniak et al., 1994; Aitchison et al., 1995*a*). Four of these—Pom152p, Nup170p, Nup157p, and Nic96p—have been previously characterized (Grandi et al., 1993; Wozniak et al., 1994; Aitchison et al., 1995*a*). In addition to these polypeptides, two major protein species were observed, both with an apparent molecular mass of ~170 kD. Using internal peptide sequence information from the faster migrating band (Fig. 1 *A*), we cloned the *NUP188* gene from a yeast genomic library as two overlapping clones that defined a 1655–amino acid residue ORF with a deduced mass 188,459 D. We have termed this gene *NUP188*, using conventional nucleoporin nomenclature. Deletion of the entire *NUP188* ORF in a yeast haploid strain did not affect the growth of this strain at temperatures ranging from 16 to 37°C (see Materials and Methods; data not shown) or its nuclear morphology (see Fig. 5). This phenotype is similar to that observed in null mutations of *POM152*, *NUP170*, and *NUP157*.

A fusion protein containing amino-acid residues 1041–1613 of Nup188p was used to produce antibodies in rabbits which were found to react specifically with Nup188p (Fig. 1 *A*). A Western blot of sucrose gradient fractions derived from the yeast NPC isolation procedure revealed that Nup188p cofractionated absolutely with isolated NPCs (Fig. 1 *B*). We epitope tagged either full-length *NUP188* or a truncated form of *NUP188* ending at residue 1313 by fusing a DNA fragment encoding the IgG-binding domain of *S. aureus* protein A to the *NUP188* carboxyl-terminus. When analyzed for their ability to complement an inactive *nup188* gene in a synthetically lethal background (see below), the full-length fusion protein (Nup188PAp), but not the truncated version (Nup188BPAp), was found to be fully functional (data not shown). The subcellular distributions of both fusion proteins were examined by indirect immunofluorescence. Nup188PAp (full-length Nup188p-prot A) was visible in a punctate pattern on the surface of the nucleus, characteristic of its localization to the NPC (Fig. 1 *C*). However, Nup188BPAp (truncated Nup188p) was primarily visible in the cytosol (Fig. 1 *C*). These data suggest that the carboxyl-terminal domain of Nup188p is necessary for the localization to the NPC.

Nup188p Is Associated with the NPC Core

Nuclear envelopes isolated from the protein A–tagged Nup188p strain (NP188PA) were probed with purified

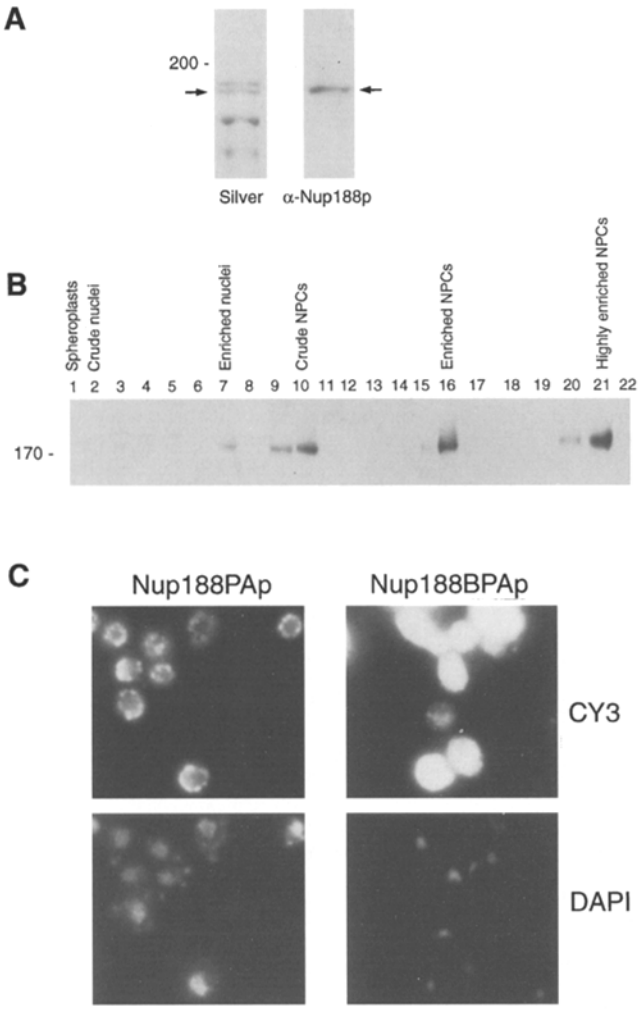

Figure 1. Nup188p is a nucleoporin. (*A* and *B*) Identification of Nup188p as a major constituent of isolated yeast NPCs. In *A*, polypeptides in a fraction containing a doublet of ~170 kD (derived from SDS-hydroxylapatite chromatography of isolated yeast NPC, see Wozniak et al. [1994], Fig. 3, fractions 43–45) were separated on an SDS 8–5% inverse polyacrylamide gradient gel and visualized by silver staining (*Silver*). The faster migrating species of the doublet (*arrow*) was microsequenced, its gene was cloned, and the protein was termed Nup188p. Western blots were performed on identical fractions using an antibody directed against Nup188p (α-*Nup188p*). In *B*, protein constituents of fractions derived from the sequential sucrose gradients used in the enrichment of yeast NPCs were separated by SDS-PAGE and Western blotted with antibodies directed against Nup188p. The number of starting cell equivalents per lane is exactly as defined in Fig. 1 of Wozniak et al. (1994). Nup188p coenriched with the NPCs. Molecular mass markers are indicated in kilodaltons. (*C*) Localization of Nup188p and Nup188Bp tagged with protein A. Full-length Nup188p (*Nup188PAp*) and a carboxyl-terminal truncated Nup188p (*Nup188BPAp*) fused to the IgG-binding repeats of *Staphylococcus* protein A were localized by indirect immunofluorescence of whole yeast cells using rabbit anti–mouse IgG, followed by donkey anti–rabbit coupled to the fluorescent tag Cy3. Nup188PAp (full-length Nup188p) gives punctate NE staining, while truncated Nup188p (Nup188BPAp) localizes mainly to the cytoplasm. Corresponding 4′,6-diamidino-2-phenylindole (DAPI) staining of DNA is shown below.

rabbit antibody, and the binding was visualized with gold-labeled secondary antibody by electron microscopy. As has been previously demonstrated with Nup159p (Kraemer et al., 1995), the use of a preembedding immunolabeling technique made it possible to sublocalize Nup188p on the yeast NPC with greater accuracy than the previously used postembedding labeling methods (Fig. 2 *A*). The distance from the center of each gold particle (165 particles total) to the midplane of its associated NPC was measured for 104 NPCs clearly sectioned perpendicular to that plane (and hence to the plane of the NE) (Fig. 2 *B*). The gold was distributed equally on both the nucleoplasmic and cytoplasmic faces (Fig. 2, *A* and *B*). Most particles were found within 20 nm of the midplane of the NPC (20 ± 13 nm, n = 80, on the nucleoplasmic side; 18 ± 12 nm, n = 85, on the cytoplasmic side) (Fig. 2 *B*). Many NPCs were multiply labeled, both on the same face and on opposite faces (Fig. 2 *A*). Unfortunately, without three-dimensional reconstruction, the radial distribution of the gold cannot be as reliably quantified; however, many particles were apparently located close to the cylindrical axis of the NPC (Fig. 2 *A*).

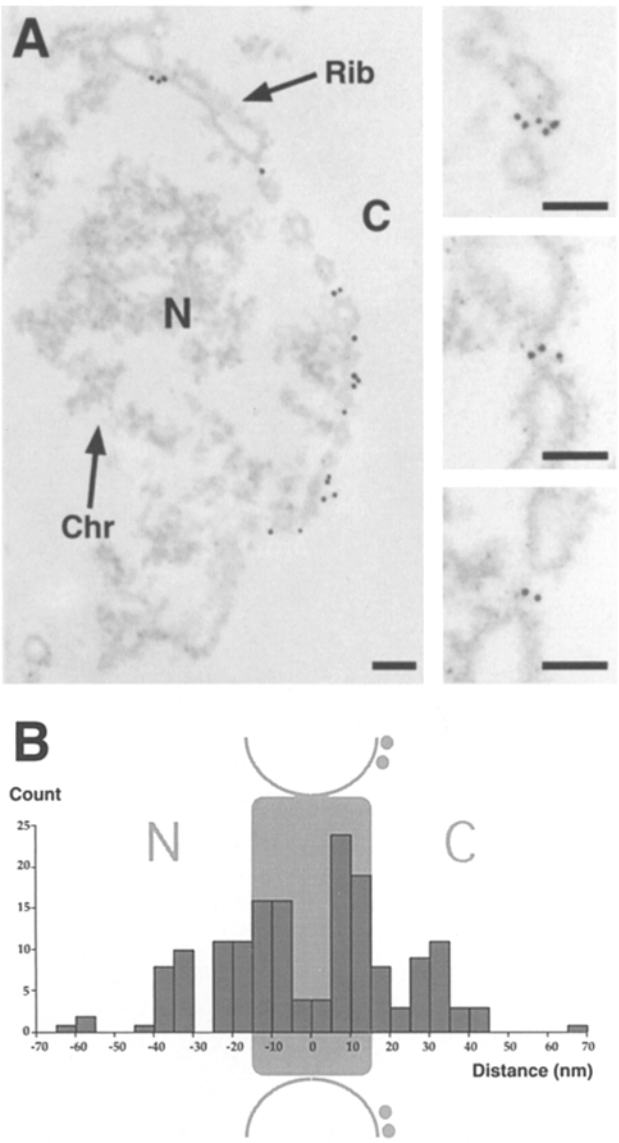

Figure 2. Nup188p is symmetrically distributed on both faces of the NPC. (*A*) Localization of protein A–tagged Nup188p in isolated NEs, as visualized by the binding of rabbit IgG and gold-labeled secondary antibodies. The nuclear side of the envelope (*N*) is on the concave face with attached chromatin (*Chr*); the cytoplasmic face (*C*) reveals associated ribosomes (*Rib*). Nup188p appeared to be present in multiple copies and accessible from both sides of the NE, close to the central cylindrical axis of the NPCs. Bar, 0.1 μm. (*B*) Histogram quantification of the distribution of 165 gold particles on the NEs (*count*), measured as the distance (*Distance (nm)*) from the center of each gold particle to the midplane of its associated NPC. Particles to the cytoplasmic side of this midplane have positive distances, while particles to the nucleoplasmic side have negative distances. Most particles were found within 20 nm of either face of the NPC. A diagrammatic silhouette of a yeast NPC (drawn to scale) has been placed behind the histogram for reference.

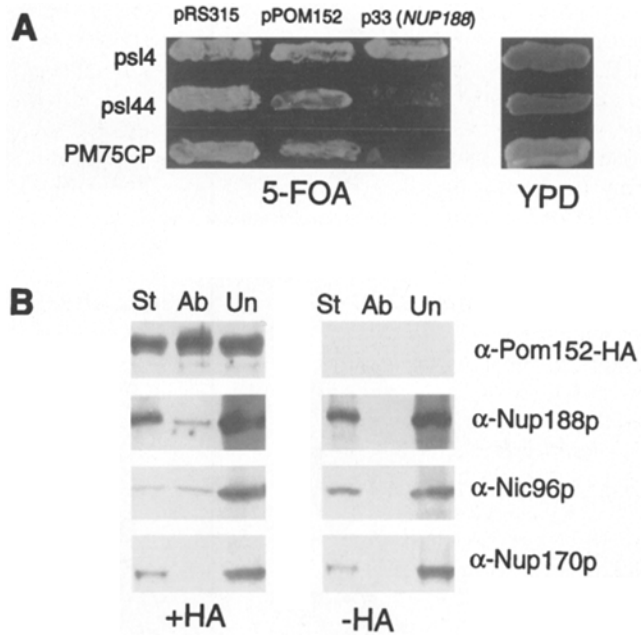

Figure 3. Nup188p interacts genetically and physically with Pom152p. (*A*) The mutant strains psl4 and psl44 and parental strain PM152-CP (Aitchison et al., 1995*a*; PM75CP) were grown on 5-FOA–containing or YPD plates for 3 d at 30°C. The growth of each strain on 5-FOA was evaluated after the introduction of the plasmids containing *POM152* (pPOM152), *NUP188* (p33), or a control plasmid without insert (pRS315). Both psl4 and psl44 containing pRS315 fail to grow on 5-FOA. Growth on 5-FOA can be restored to both mutants by *POM152* or *NUP188*. (*B*) NEs isolated from a strain expressing HA-tagged Pom152p (P7AB-B61H; *+HA*) and a strain expressing untagged Pom152p (P7AB-1; *−HA*) were extracted with Triton X-100–containing buffer and centrifuged. The supernatant fractions derived from both strains were immunoprecipitated with the anti-HA mAb 12CA5. Polypeptides in the initial supernatant fraction (Sp; 1 equivalent), the immunoadsorbed fraction (*Ab*; derived from 25 Eq of Sp), and the unbound fraction (*Un*; derived from 7.5 Eq of Sp) were separated by SDS-PAGE, transferred to nitrocellulose, and probed with antibodies directed against the HA tag (*α-Pom152p-HA*), Nup188p (*α-Nup188p*), Nic96p (*α-Nic96p*), and Nup170p (*α-Nup170p*). In each case the relevant region of the blot is shown. Nup188p and Nic96p, but not Nup170p, coimmunoprecipitated with Pom152p. None of these proteins were immunoprecipitated from the control strain lacking the HA tag (*−HA*).

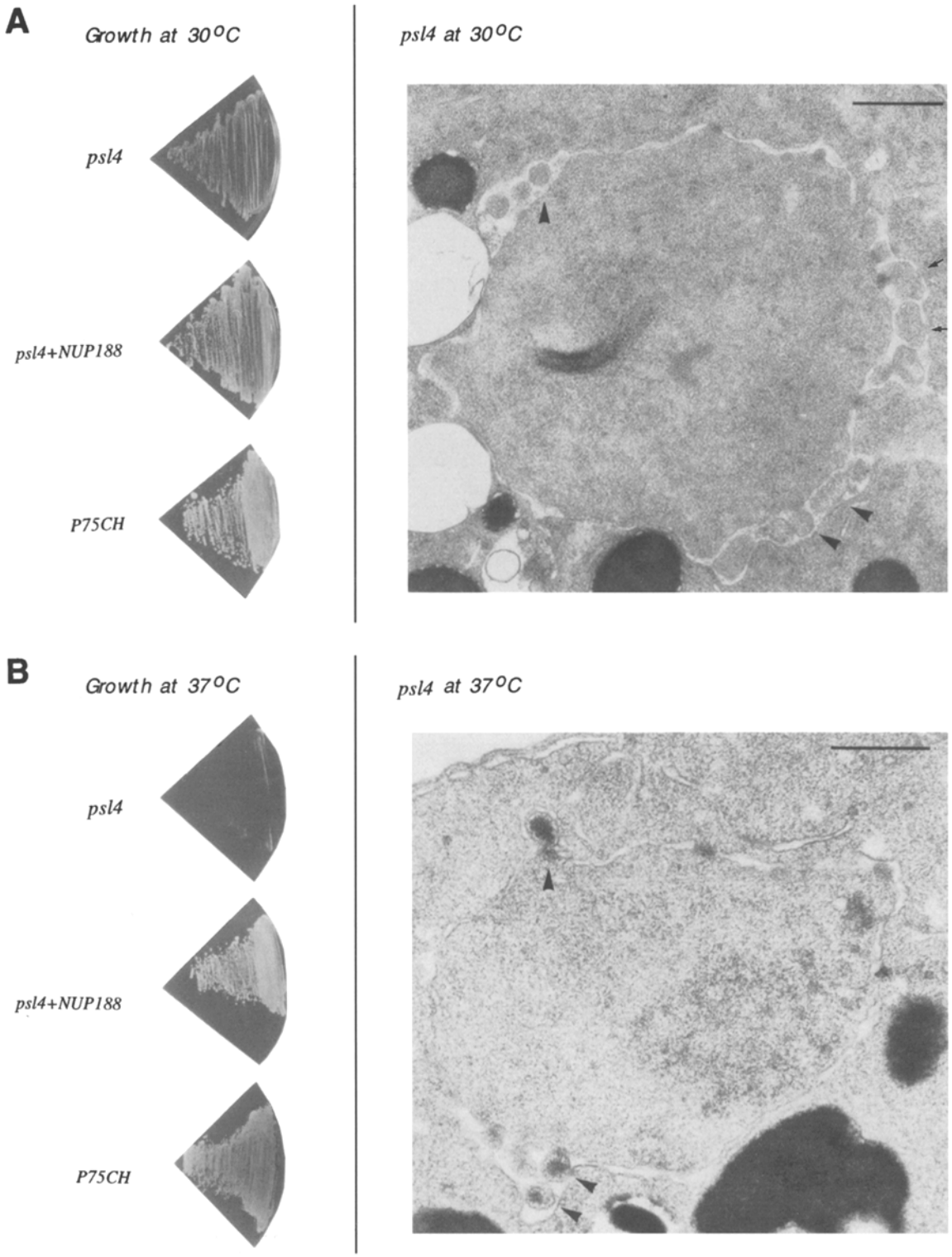

Figure 4. Psl4 cells reveal a temperature-sensitive growth defect and NPC-associated herniations. (*A*) The psl4 strain (*psl4*), the psl4 strain containing the plasmid p33 (*NUP188*)(*psl4+NUP188*) and parental strain PM152-CP (*P75CH*) were grown on YPD plates for 3 d at 30°C (*left*). Only slight differences in the growth rates of the respective strains can be observed. Shown on the right is an electron micrograph of a thin-sectioned psl4 cell grown at 30°C in YPD. NPC-associated NE herniations are marked by arrowheads. Arrows point to fenestrations often visible in the herniations. (*B*) Shown on the left are the strains described in *A* grown on YPD plates for 3 d at 37°C. A significant delay in the growth rate of the psl4 strain can be observed at 37°C (*psl4*). This ts phenotype could be complemented by wild-type *NUP188* (*psl4+NUP188*). Shown on the right is an electron micrograph of a thin-sectioned psl4 cell grown at 37°C for 9 h. NPC-associated NE herniations are marked by arrowheads. At this temperature, some herniations appear filled with electron-dense material. Bar, 0.5 μm.

Taken together, these data indicate that Nup188p–protein A is present in multiple copies and accessible on both faces of the NPC. Assuming that this localization reflects the position of the protein bulk, these data suggest that Nup188p is associated with the NPC core, perhaps as a component of the inner-spoke domain or the central transporter.

Nup188p Interacts Genetically and Physically with Pom152p

The *NUP188* gene was also identified in a colony-sectoring assay designed to identify genes that are synthetically lethal with *POM152* (for details see Materials and Methods and Aitchison et al., 1995*a*). Of the 32 recessive, nonsectoring mutants (termed psl mutants) obtained in this screen, 20 were allelic to *NUP188*. As shown in Fig. 3 *A*, two synthetically lethal mutants, psl4 and psl44, regained the ability to grow on 5-FOA medium and to sector on YPD medium after transformation with either the *POM152* or *NUP188* gene. Consistent with this observed synthetic lethality, a haploid strain lacking both the *POM152* and the *NUP188* genes was not viable (data not shown). The remaining 12 mutants originally obtained in the screen, which were not complemented by *NUP188*, fell into three other complementation groups; one set allelic to the major nucleoporin gene *NUP170* (Aitchison et al., 1995*a*), a second set could be rescued by the nucleoporin Nic96p, and a third by an as yet uncharacterized plasmid termed p40 (M. Marelli and R.W. Wozniak, unpublished results).

The genetic interactions between *POM152* and *NUP188* suggested an overlapping role for these proteins in NPC function and/or their physical interaction. In an effort to determine whether in fact Pom152p and Nup188p physically interact, we performed immunoprecipitations on nuclear envelope extracts derived from strains synthesizing HA-tagged Pom152p (Pom152p-HA). Nuclear envelopes were disrupted under conditions that release the majority of Pom152p-HA (~80%) into a soluble supernatant fraction after centrifugation (data not shown). Pom152p-HA was immunoprecipitated from this fraction using an mAb (12CA5) specific for the HA epitope. Analysis of the immunoabsorbed fraction by Western blotting revealed that Nup188p and Nic96p, but not Nup170p, were coimmunoprecipitated with Pom152p-HA (Fig. 3 *B*, *+HA*). None of these proteins were detected in parallel immunoprecipitates derived from the strain lacking HA-tagged Pom152p (Fig. 3 *B*, *−HA*). These data suggest that Pom152p is physically associated, either directly or indirectly, with Nup188p and Nic96p in an NPC subcomplex lacking Nup170p. We note that a major portion of Pom152p-HA, Nup188p, and Nic96p are not immunoprecipitated with the 12CA5 mAb, suggesting that this complex may be largely inaccessible to the antibody and/or unstable under the conditions we have used to dissociate it from the NE.

A nup188p Mutant, psl4, Reveals Structural Abnormalities of the NE without Affecting Nuclear Transport

We have examined the growth of a *nup188* mutant strain, *psl4* (see Fig. 3 *A*), at various temperatures ranging from 23° to 37°C. While the doubling time of the psl4 cells at 30°C (2.4 h) was only slightly slower than the PM152-75 parent strain (2.1 h), growth was inhibited at 37°C (Fig. 4 *B*, *left panel*). This growth defect could be rescued by introducing wild-type *NUP188* (Fig. 4 *B*, *left panel*). Mutant cells (psl4) were either maintained at 30°C or shifted to 37°C for 9 h and then processed for thin-section electron microscopy. At both temperatures, the morphology of the nucleus and NE appeared essentially identical (Fig. 4, *A* and *B*, *right panels*), with many NPCs being enclosed on their cytoplasmic face by NE herniations similar to structures previously described by Wente and Blobel (1993). No apparent increase in the frequency of the NPC-associated herniations was observed in cells grown at 37°C. Cells grown at 37°C, but not those grown at 30°C, contained electron-dense material within several of these herniations (Fig. 4, *A* and *B*, *right panels*). This would suggest that at 37°C, the herniations are accumulating material being exported from the nucleus. However, when mRNA export was analyzed at both 30°C and 37°C by in situ hybridization using oligo-dT, no apparent accumulation of mRNA in the nucleus or at the nuclear periphery could be detected at either temperature (data not shown). Also, nuclear import, as monitored by the subcellular distribution of the nuclear protein NSR1 (Lee et al., 1992), was not affected at either temperature (data not shown).

Pom152p Depletion in a nup188Δ Genetic Background Leads to Structural Distortions of the Nucleus

The effects of the conditional lethality observed between the *NUP188* and *POM152* null mutants on the structure of the nucleus were examined in a genetic background lacking the chromosomal copies of *POM152* and *NUP188*, but carrying the *POM152* gene, under the control of the regulatable *GAL1* promoter in the plasmid pYEUra3 (*URA3*). The viability of the resulting *GAL1::pom152*, *nup188Δ* mutant strain, CSL5, was expected to be dependent on *GAL1*-controlled *POM152* expression. When we analyzed the growth rate of the CSL5 strain, we observed a significant increase in the doubling time upon a shift to glucose-containing medium (2.2 h in galactose to 5 h in glucose). Surprisingly, even after 30 h of growth in glucose, CSL5 cells were still viable. The survival of the CSL5 strain in glucose medium after 30 h was most likely caused by incomplete repression of the *GAL1* promoter. This is supported by Western blots of CSL5 cells grown for up to 30 h in glucose, in which detectable amounts of Pom152p were visible (Fig. 5 *A*). The low level of *Pom152p* detectable after a 30-h depletion was apparently sufficient to support slow growth.

When examined for morphological changes, CSL5 cells grown in galactose appeared normal (Fig. 5 *C*, *+Galactose*). However, after 30 h depletion of Pom152p in glucose medium, the shape of the nucleus became severely distorted, losing its rounded shape (Fig. 5 *D*, *+Glucose*). Projections of the NE were visible extending into the cytosol. In addition, the NE appeared to form extensive invaginations into the nucleus. These distortions in the shape of the nuclear envelope are similar to those that were previously observed upon depletion of Nup170p in cells lacking Pom152p (Aitchison et al., 1995*a*). Unlike the Nup170p depleted strain, however, we observed no apparent decrease in the number of NPCs.

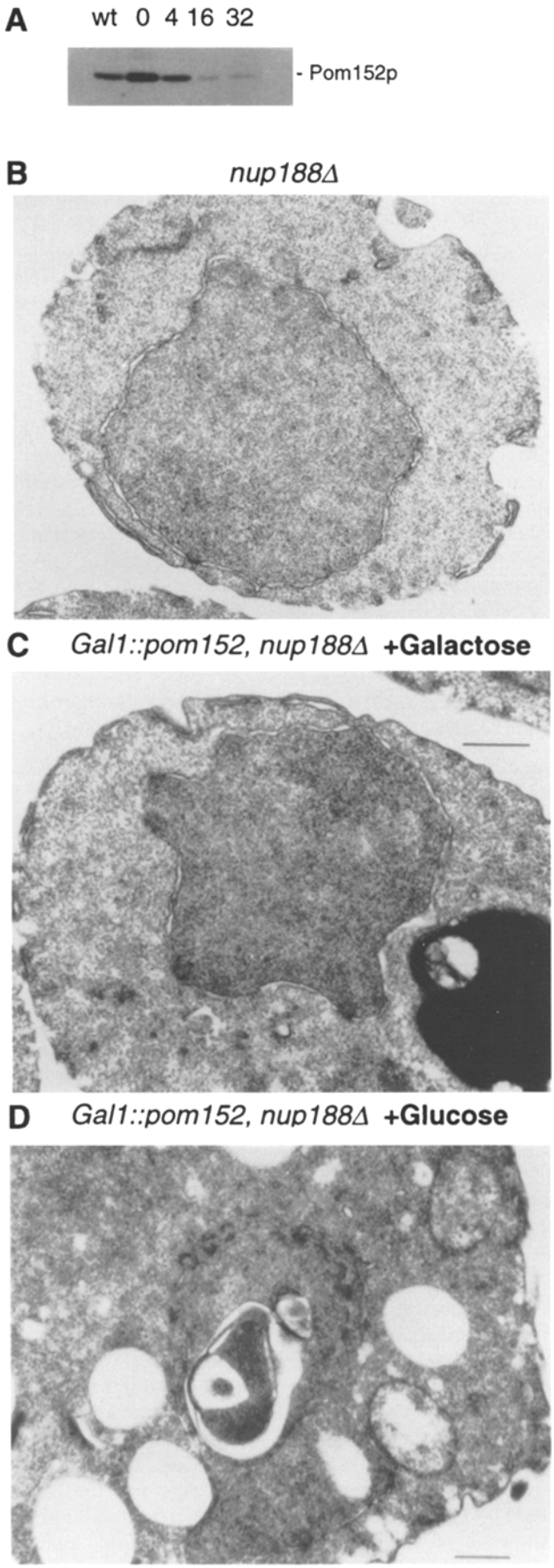

Discussion

Nup188p belongs to a subgroup of NPC constituents that do not contain peptide repeat motifs and together constitute a significant percentage of the NPC mass. We refer to this subgroup of nucleoporins as "major nonrepeat nucleoporins." This classification goes beyond a descriptive level, since the other members of this subgroup, including Nup170p, Nup157p, and Nic96p, have previously been shown to genetically interact with each other and Pom152p (Aitchison et al., 1995*a*; Zabel et al., 1996). This genetic interaction has its basis in either a physical interaction and/or an overlap in the respective functions of these proteins. Accordingly, Nup188p was identified both as a major protein in a highly enriched pore complex preparation and as a mutant that is synthetically lethal with Pom152p.

The localization of Pom152p to the pore membrane domain established it as a constituent of the NPC core (Wozniak et al., 1994). Nup188p can be assigned to the same NPC substructure. Using immunoelectron microscopy, Nup188p was found symmetrically distributed at both cytoplasmic and nucleoplasmic faces of the NPC. The close proximity of the gold label to the central plane of the NPC strongly suggests that Nup188p is a component of the NPC core, most likely the spokes or the central transporter. Moreover, using HA-tagged Pom152p, Nup188p could be specifically immunoprecipitated from NEs using HA antibodies, demonstrating that these proteins are physically associated. Thus, Pom152p and Nup188p are two major constituents of the NPC core domain that interact both physically and genetically. Interestingly, these interactions also extend to other major nonrepeat nucleoporins. As can be seen from Fig. 3 *B*, Pom152p also appears associated with Nic96p, and in an accompanying study by Zabel et al. (1996), Nup188p was shown to interact with Nic96p. A physical interaction between Pom152p and Nic96p is consistent with previous data showing their genetic interactions (Aitchison et al., 1995*a*). These results strongly suggest that the genetic interactions between major nonrepeat nucleoporins are based on their physical interaction. It is therefore conceivable that this entire subgroup of major

Figure 5. Pom152p depletion in a nup188Δ background results in structural distortions of the nucleus. (*A*) The depletion of Pom152p in the CSL5 strain after shift to glucose-containing medium. Equivalent amounts of cells derived from the CSL5 strain grown in galactose medium (0) or 4 h (4), 16 h (16), and 30 h (30) after the shift to glucose-containing medium were extracted and solubilized in SDS-containing buffer. Polypeptides were separated by SDS-PAGE and immunoblotted using an mAb directed against Pom152p. Blots of an equivalent amount of W303 cells grown in YPD medium is also shown (*wt*). (*B–D*) Thin-section electron micrographs of strains lacking NUP188. A *nup188* null strain (NP188-2.4) expressing wild-type levels of *POM152* is shown in *B* (*nup188Δ*). No structural abnormalities in the nucleus and nuclear envelope are visible in this strain. (*B* and *C*) Thin-sectioned CSL5 cells (*GAL1::pom152, nup188Δ*) grown in galactose-containing medium (+*Galactose*) at 30°C or in glucose-containing medium (+*Glucose*) for 30 h at 30°C. CSL5 cells grown in galactose reveal normal nuclear morphology (*C*). Growth in glucose (low levels of *POM152* expression) leads to a loss of the rounded nuclear morphology, as well as the appearance of prominent projections and invaginations of the NE (*D*). Bars, 0.5 μm.

nucleoporins is involved in forming a common NPC substructure, such as the octagonal core, with its repetitive spoke, ring, and radial arm structures.

A role of Nup188p in the structural organization of the NPC core should ideally correlate with structural NPC defects of *nup188* mutants in vivo. One *nup188* mutant allele analyzed for morphological abnormalities is *psl4*. It exhibited a temperature-sensitive phenotype that could be rescued by wild-type *NUP188*. This growth defect is in contrast to a *nup188* null mutation that showed no growth abnormalities. Thus, it is likely that the product of the *psl4* allele is more detrimental to NPC function than the complete removal of the wild-type protein. An examination of the morphology of the NE in the psl4 strain at 30° and 37°C revealed the presence of NPC-associated NE herniations similar to those observed in *nup116* null mutations at restrictive temperatures (Wente and Blobel, 1993). In contrast to the *NUP116* mutants, however, the herniations seen in Fig. 4 were free of electron-dense material at 30°C, and revealed such accumulation only at 37°C. Although this material in the herniations may represent some trapped nuclear transport cargo, no significant inhibition of nuclear transport could be detected in psl4 cells at either temperature (data not shown). The *nup188* mutant in psl4 therefore appears to primarily affect the structural organization of the NPC rather than having a direct impact on nuclear transport mechanisms.

Upon depletion of a second NPC core component, Pom152p, in cells already lacking Nup188p, structural distortions of the nucleus became more profound. They were no longer confined to the area of the NPC, but rather affected the structural integrity of the whole nuclear envelope. As shown in Fig. 5, the gradual depletion of Pom152p in cells lacking Nup188p led to severe distortions in the shape of the nucleus which are visible as extended projections and invaginations of the NE. It is unlikely that these structural distortions of the NE are the pleiotropic result of dying cells, since the depletion of Pom152p was not complete and the cells continued to grow. Again, the persistence of growth implies a continuation of nuclear transport mechanisms despite a highly compromised NE structure.

Taken together, these experiments suggest that Nup188p is a component of the NPC core and has an important role in the structural organization of the NPC and the NE. We hypothesize that Nup188p, as well as the other major nonrepeat nucleoporins and Pom152p, represent a subgroup of NPC proteins that help to constitute the core of the NPC. This core may represent the structural framework that is required for the correct positioning of repeat nucleoporins and other NPC components directly involved in nuclear transport mechanisms. The only major nonrepeat nucleoporin shown to undergo genetic and physical interactions with repeat nucleoporins is Nic96p (interacting with Nsp1p, Nup49p, and Nup57p [Grandi et al., 1995]). In the context of data presented in this paper and Zabel et al. (1996), Nic96p could therefore link this repeat nucleoporin subcomplex to the NPC core, effectively connecting the elements of the transport machinery to the structural framework of the NPC and, via Pom152p, to the pore membrane domain.

We thank The Rockefeller University/Howard Hughes Medical Institute Biopolymer Facility, especially Joseph Fernandez, for oligonucleotide synthesis and peptide sequencing; Eleana Sphicas for assistance in performing the electron microscopy studies; Dr. Ed Hurt for sharing unpublished information and the anti-Nic96p antibodies; Drs. John Aitchison and Felix Kessler for helpful discussion. R.W. Wozniak is an Alberta Heritage Scholar.

This work was supported in part by an operating grant from the Medical Research Council of Canada.

Received for publication 14 September 1995 and in revised form 8 March 1996.

References

Aitchison, J.D., M.P. Rout, M. Marelli, G. Blobel, and R.W. Wozniak. 1995*a*. Two novel related yeast nucleoporins Nup170p and Nup157p: complementation with the vertebrate homologue Nup155p and functional interactions with the yeast nuclear pore-membrane protein Pom152p. *J. Cell Biol.* 131: 1133–1148.

Aitchison, J.D., G. Blobel, and M.P. Rout. 1995*b*. A yeast nucleoporin required for NPC distribution and mRNA transport. *J. Cell Biol.* 131:1559–1675.

Akey, C.W., and M. Radermacher. 1993. Architecture of the *Xenopus* nuclear pore complex revealed by three dimensional cryo-electron microscopy. *J. Cell Biol.* 122:1–19.

Ausubel, F.M., R. Brent, R.E. Kingston, D.D. Moore, J.G. Seidman, F.A. Smith, and K. Struhl. 1992. Short protocols in molecular biology. Greene Publishing Associates, New York. 312–315.

Doye, V., R. Wepf, and E.C. Hurt. 1994. A novel nuclear pore protein Nup133p with distinct roles in poly(A)$^+$ RNA transport and nuclear pore distribution. *EMBO (Eur. Mol. Biol. Organ.) J.* 13:6062–6075.

Fabre, E., and E.C. Hurt. 1994. Nuclear transport. *Curr. Opin. Cell Biol.* 6:335–342.

Goldberg, M.W., J.J.Blow, and T.D. Allen. 1992. The use of field emission inlens scanning electron microscopy to study the steps of assembly of the nuclear envelope in vitro. *J. Struct. Biol.* 108:257–268.

Goldberg, M.W., and T.D. Allen. 1995. Structural and functional organization of the nuclear envelope. *Curr. Opin. Cell Biol.* 7:301–309.

Gorsch, L.C., T.C. Dockendorff, and C.N. Cole. 1995. A conditional allele of the novel repeat-containing yeast nucleoporin *RAT7/NUP159* causes both rapid cessation of mRNA export and reversible clustering of nuclear pore complexes. *J. Cell Biol.* 129:939–955.

Grandi, P., V. Doye, and E.C. Hurt. 1993. Purification of NSP1 reveals complex formation with 'GLFG' nucleoporins and a novel nuclear pore protein NIC96. *EMBO (Eur. Mol. Biol. Organ.) J.* 12:3061–3071.

Grandi, P., N. Schlaich, H. Tekotte, and E.C. Hurt. 1995. Functional interaction of Nic96p with a core nucleoporin complex consisting of Nsp1p, Nup49p and a novel protein Nup57p. *EMBO (Eur. Mol. Biol. Organ.) J.* 14:76–87.

Heath, C.V., C.S. Copeland, D.C. Amberg, V. Del Piore, M. Snyder, and C.N. Cole. 1995. Nuclear pore complex clustering and nuclear accumulation of poly(A)$^+$RNA associated with mutation of the *S. cerevisiae RAT2/NUP120* gene. *J. Cell Biol.* 131:1677–1697.

Hinshaw, J.E., B.O. Carragher, and R.A. Milligan. 1992. Architecture and design of the nuclear pore complex. *Cell.* 69:1133–1141.

Hurwitz, M.E., and G. Blobel. 1995. *NUP82* is an essential yeast nucleoporin required for poly(A)$^+$RNA export. *J. Cell Biol.*

Iovine, M.K., J.L. Watkins, and S.R. Wente. 1995. The GLFG repetitive region of the nucleoporin Nup116p interacts with Kap95p, an essential yeast nuclear import factor. *J. Cell Biol.* 131:1699–1713.

Jarnik, H., and U. Aebi. 1991. Toward a more complete 3-D structure of the nuclear pore complex. *J. Struct. Biol.* 107:291–308.

Jones, J.S., and L. Prakash. 1990. Yeast *Saccharomyces cerevisiae* selectable markers in pUC18 polylinker. *Yeast.* 6:363–366.

Kilmartin, J.V., and A.E.M. Adams. 1984. Structural rearrangements of tubulin and actin during the cell cycle of the yeast *Saccharomyces*. *J. Cell Biol.* 98: 922–933.

Kraemer, D.M., C. Strambio-de-Castillia, G. Blobel, and M.P. Rout. 1995. The essential yeast nucleoporin *NUP159* is located on the cytoplasmic side of the nuclear pore complex and serves in karyopherin-mediated binding of transport substrate. *J. Biol. Chem.* 270:19017–19021.

Lee, C.C., W. Xiangwei, R.A. Gibbs, R.G. Cook, D.M. Muszny, and C.T. Caskey. 1988. Generation of cDNA probes directed by amino acid sequence: cloning of urate oxidase. *Science (Wash. DC).* 239:1288–1291.

Lee, W.C., D. Zabitakis, and T. Melese. 1992. NSR1 is required for pre-rRNA processing and for the proper maintenance of steady-state levels of ribosomal subunits. *Mol. Cell Biol.* 12:3865–3871.

Li, O., C.V. Hearth, D.C. Amberg, T.C. Dockendorff, C.S. Copeland, M. Snyder, and C.N. Cole. 1995. Mutations or deletion of the *S. cerevisiae RAT3/NUP133* gene causes temperature dependent nuclear accumulation of poly (A)$^+$ RNA and constitutive clustering of nuclear pore complexes. *Mol. Biol. Cell.* 6:401–417.

Moroianu, J., G. Blobel, and A. Radu. 1995. A previously identified protein of uncertain function is karyopherin-α and together with karyopherin-β docks import substrate at nuclear pore complexes. *Proc. Natl. Acad. Sci. USA.* 92: 2088–2091.

Pemberton, L.F., M.P. Rout, and G. Blobel. 1995. Disruption of the nucle-

oporin gene *NUP133* results in clustering of nuclear pore complexes. *Proc. Natl. Acad. Sci. USA*. 62:1187–1191.

Radu, A., M.S. Moore, and G. Blobel. 1995. The peptide repeat domain of nucleoporin Nup98 functions as a docking site in transport across the nuclear pore complex. *Cell*. 81:215–222.

Rexach M., and G. Blobel. 1995. Association and dissociation reactions involving transport substrate, transport factors and nucleoporins. 1995. *Cell*. 85: 683–692.

Ris, H., and M. Malecki. 1993. High-resolution field emission scanning electron microscope imaging of internal cell structures after Epon extraction from sections: a new approach to correlative ultrastructural and immunocytochemical studies. *J. Struct. Biol*. 111:148–157.

Rose, M.D., P. Novick, J.H. Thomas, D. Bothstein, and G.R. Fink. 1987. A *Saccharomyces cerevisiae* genomic plasmid bank based on a centromere-containing shuttle vector. *Gene (Amst.)*. 60:237–243.

Rothstein, R. 1991. Targeting, disruption, replacement, and allele rescue: integrative DNA transformation in yeast. *Methods Enzymol*. 194:281–301.

Rout, M.P., and G. Blobel. 1993. Isolation of the yeast nuclear pore complex. *J. Cell Biol*. 123:771–783.

Rout, M.P., and S.R. Wente. 1994. Pores for thought: nuclear pore complex proteins. *Trends Cell Biol*. 4:357–365.

Schneiter, R., T. Kadowaki, and A.T. Tartakoff. 1995. mRNA transport in yeast: time to reinvestigate the functions of the nucleolus. *Mol. Biol. Cell*. 6:357–370.

Schnell, D.J., and G. Blobel. 1993. Identification of intermediates in the pathway of protein import into chloroplasts and their localization to envelope contact sites. *J. Cell Biol*. 120:103–115.

Strambio-de-Castillia, C., G. Blobel, and M.P. Rout. 1995. Isolation and characterization of nuclear envelopes from the yeast *Saccharomyces*. *J. Cell Biol*. 131:19–31.

Unwin, P.N., and R.A. Milligan. 1982. A large particle associated with the perimeter of the nuclear pore complex. *J. Cell Biol*. 93:63–75.

Wente, S.R., M.P. Rout, and G. Blobel. 1992. A new family of yeast nuclear pore complex proteins. *J. Cell Biol*. 119:705–723.

Wente, S.R., and G. Blobel. 1993. A temperature-sensitive NUP116 null mutant forms a nuclear envelope seal over the yeast nuclear pore complex thereby blocking nucleocytoplasmic traffic. *J. Cell Biol*. 123:275–284.

Wimmer, C., V. Doye, P. Grandi, U. Nehrbass, and E.C. Hurt. 1992. A new subclass of nucleoporins that functionally interact with the nuclear pore protein NSP1. *EMBO (Eur. Mol. Biol. Organ.) J*. 11:5051–5061.

Wozniak, R.W., G. Blobel, and M.P. Rout. 1994. POM152 is an integral protein of the pore membrane domain of the yeast nuclear envelope. *J. Cell Biol*. 125:31–42.

Zabel, U., V. Doye, H. Tekotte, R. Wepf, and E.C. Hurt. 1996. Nic96p is required for nuclear pore formation and functionally interacts with a novel nucleoporin, Nup188p. *J. Cell Biol*. 133:1141–1152.